Corrosion monitoring on steel reinforced nano metaclayed-UHPC towards strain modulation using fiber Bragg grating sensor

M F Md Jaafar[1], H Mohd Saman[2], N F Ariffin[1], K Muthusamy[1], S Wan Ahmad[1], N Ismail[3]

[1]Faculty of Civil Engineering & Earth Resources, Universiti Malaysia Pahang, Lebuhraya Tun Razak, 26300 Gambang, Pahang, MALAYSIA
[2]Faculty of Civil Engineering, Universiti Teknologi Mara Shah Alam, 40450 Shah Alam, Selangor, MALAYSIA
[3]Faculty of Civil & Environmental Engineering, Universiti Tun Hussien Onn Malaysia, 86400 Batu Pahat, MALAYSIA

faizaljaafar@ump.edu.my[1], hamid929@salam.uitm.edu.my[2], khairunsisa@ump.edu.my[1], farhayu@ump.edu.my[1], saffuan@ump.edu.my[1], noorli@uthm.edu.my[3]

Abstract. Today, research on steel corrosion issues are still widely debated and revived scientific attention. In order to detect steel corrosion, an idea to explore the relationship of corrosion potential using half-cell potential related to the variations in strain change on embedded steel measured by FBG sensor were explored. In this study, the steel was embedded in various types of concrete consist of NPC, HPC, UHPC and a series of nano metaclayed-UHPC. It was observed that the steel embedded in NPC is very low in corrosion resistance. Conversely, nano metaclayed-UHPC can delay the embedded steel to corroded. It was also noticeably that the corrosion readings for steel embedded in NPC specimens possess the highest possibility of corrosion potential as well as the large strain was observed by using FBG. Inclusion of 1% nano metaclay in UHPC shows a superior performance in term of corrosion resistance and protected the steel from corrosion. The RSM analysis was found that the R^2 values are strong relationship between corrosion potential and strain changes. The R^2 obtained for NPC, HPC, UHPC, UHPC1, UHPC3 and UHPC5 models associated with corrosion potential with respect to strain changes were found to be 0.95, 0.99, 0.87, 0.93, 0.98 and 0.97, respectively.

1. Introduction

Corrosion of steel reinforced concrete structures is one of the most frequent reasons for civil infrastructure failures [1]. Monitoring on reinforcement corrosion via well-established methods presently relies on physical deterioration of reinforced concrete structure [2-4]. The method demonstrated lack of precision in visual inspection for early stage of detecting corrosion for embedded steel. On the other hand, most of the conventional techniques are electrochemical in mechanisms. Several methods such as potential measurement, polarization resistance measurement and electrochemical impedance have also been widely used for monitor the corrosion activity on steel embedded in concrete

[5-8]. In some situation, this method records unreasonable results and the degree of reinforcement corrosion cannot be directly depicted. Therefore, the need to improve the effective corrosion technology can greatly provide early detection on steel corrosion. It is proposed that the change of strain surrounding steel reinforcement in concrete could be used to verify the corrosion potential measured conventional techniques [9]. Fundamentally, when the embedded reinforcement starts to corrode, the steel surface becomes oxidized resulting the reduction in cross sectional area of steel due to expanded volume of corrosion product. The strain region of steel can be an indicator of the corrosion initiation. Nowadays, interests in using kinds of novel sensors namely fiber Bragg grating (FBG) in structure monitoring have increased significantly. FBG has a great potential to allows strain measurement to be made in situations where the conventional strain gauge unattainable to monitor. Thus, FBG sensor promising features in term of high accuracy, real time measurement and small size [10-11].

Generally, FBG is spectral filters that present a resonance at the Bragg wavelength, whose value depends on the effective refractive index of the core and on the grating pitch [12]. This study provides the quantitative data on strain change recorded by FBG and how it governs the corrosion potential of steel reinforcement embedded in concrete measured by standard half-cell potential. The use of FBG applied to steel rebar embedded in concrete has been remarkable on corrosion prediction and the related research has been reported extensively. It has been revealed that the expansion on the cross-section of steel reinforcement due to corrosion was reflected to the increase of the wavelength shift recorded by FBG [13-15]. This was confirmed by [16-17] who measured the strain in corroded steel rebar of reinforced concrete using FBG and correlate with weight loss rate of corroded steel. The experiment shows that the increases of FBG wavelength shifted is reflected to the expansion of corroded steel. This is reasonable to monitor corrosion of steel in reinforced concrete structures using FBG. In the past few years, numerous successful researches were also established that the change of wavelength shifted by FBG contribute to the strain change of expansion on steel corroded [18-20]. This finding appears that FBG is one of the technique can be exploited as early corrosion detection based sensing system for prediction and monitoring the corrosion activity of steel.

In comparison to previous studies, the needs to assessing the corrosion activity of steel reinforcement embedded in ultra-high performance concrete (UHPC) offers an ideal to this study. From the ongoing, it become necessary to embark on more research on the usage of the FBG sensor for early warning detection of steel corrosion in modern concrete such as UHPC. This will contribute to new knowledge and perhaps will filled the gap of study. The strain changes of corroded steel embedded in concrete using FBG was correlate with corrosion potential measured by half-cell potential.

2. Experimental Programme

2.1. Mix proportion

The basic components of cement, coarse aggregate, sand, water and superplasticiser were mixed together by using dry mix method. In this study, six (6) series of concrete mix proportion were prepared. The concretes were classified as normal performance concrete (NPC), high performance concrete (HPC), ultra-high performance concrete (UHPC) and nano metaclayed-UHPC incorporating three (3) different levels of nano metaclay as cement replacement. The different replacement levels of nano metaclay comprised of 1, 3 and 5% from the total weight of ordinary Portland cement used. The commercially available nano clay powder (hydrophilic bentonite) was procured from Sigma-Aldrich (M) Sdn. Bhd. The raw nano clay samples were heated at the temperature of 700°C for 3 hours' process period. The calcination process is required for making the nano clay samples become reactive thus can react chemically with traditional cement. On the other hand, 10% silica fume was replaced as a cementitious material for HPC production. Table 1 shows the details of each concrete mix design. The water to cement ratio for NPC, HPC and UHPC are 0.50, 0.33 and 0.20, respectively.

Table 1. Series of mix proportion for NPC, HPC, plain UHPC and Nano Metaclayed-UHPC containing different level of nano metaclay replacement.

Mix Designation	Raw Materials (kg/m^3)						
	Portland Cement	Silica Fume	Nano Metaclay	Aggregate	Sand	Water	SP
NPC	380	-	-	995	815	190	2.85
HPC	416	46	-	1149	619	152	4.20
Plain UHPC	800	-	-	433	800	160	11.52
UHPC1	797	-	3	433	800	160	6.70
UHPC3	776	-	24	433	800	160	6.98
UHPC5	760	-	40	433	800	160	7.60

2.2. Preparation of FBG sensor embedded in reinforced concrete

FBG sensors for strain was fabricated and supplied by Photronix Technologies (M) Sdn. Bhd., Selangor. The high yield strength steel reinforcement as conform to steel structural ASTM-A36 with nominal diameter of 12 mm was used. The reinforced concrete specimens contain a centrally embedded with a single steel reinforcement of 300 ±5 mm in length with a cover about 40 ±2 mm on the both sides were prepared. The dimension of reinforced concrete specimen is 100 mm in diameter and 250 mm in height. Prior to embedding FBG sensors in reinforced concrete specimen, the FBG strain sensor was attached near to steel reinforcement using adhesive. Then, the sensors were protected by applying silicone gel. Figure 1 depicts the setup for FBG sensors on steel reinforcement and wavelength measurement using FBG interrogation system. Before immersion process, the top and bottom parts of specimen was coated using water-based PU bituminous waterproofing membrane to prevent the surface from exposure site. In addition, the exposed steel reinforcement was covered using plastic wrapping to preclude the steel rebar directly contact with environment. Subsequently, the reinforced concrete specimens attached with FBG sensor was immersed in 3% NaCl solution after cured in water for 7 days. During the immersion process, all the specimens were submerged with constant depth of 50 ±2 mm from the solution surface and the monitoring activities were conducted up to 1-year. The results obtained were simultaneously recorded by using FBG sensors and half-cell potential. All the data obtained was performed and analysed statistically using Design Expert software to establish the possible relationship. For this purpose, Response Surface Methodology (RSM) model was adopted in optimising experimental data obtained.

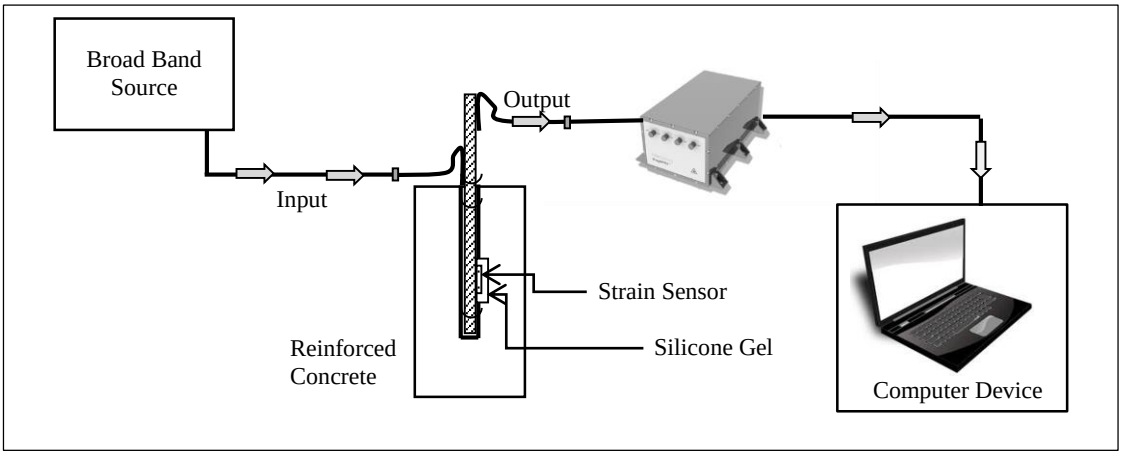

Figure 1. Setup for wavelength measurement embedded FBG sensors using FBG interrogation system.

3. Results and Discussions

3.1. Corrosion monitoring by using half-cell potential

In this study, two (2) methods of corrosion monitoring on steel embedded in NPC, HPC, UHPC and a series of nano metaclayed-UHPC is presented. The method of corrosion monitoring was measured by half-cell potential and FBG sensor. The trend of corrosion potential recorded by half-cell potential for different types of concrete with respect to age is presented in Figure 2. It was found that the potential readings for entire concrete specimens were increase in negative readings with increasing time of exposure in 3% NaCl solution. It was observed that the steel embedded in NPC specimen is very low in corrosion resistance thus the corrosion progress for embedded steel developed rapidly. Conversely, concrete composed from UHPC and nano metaclay based UHPC can delay the embedded steel to corroded as compared to that NPC and HPC specimens. The results also indicated that UHPC containing 1% nano metaclay shows a superior performance in term of corrosion resistance and protected the steel from corrosion. This would be appeared that the variation amount of nano metaclay in UHPC is more significant in their effective porosities and in the same time the strength properties enhanced. This agreed with the study on several researchers which concluded a dense concrete that containing pozzolanic cement provides a good physical barrier protecting the steel from corrosion [21-23]. On the other hand, several researchers also supported that as concrete strength increased, corrosion rate of embedded steel decreased [24,25]. It was indicated a concrete containing pozzolanic material as replacement of OPC is durable and possess minimum porosity thus improves resistance to chloride attack and better corrosion protection [26-29].

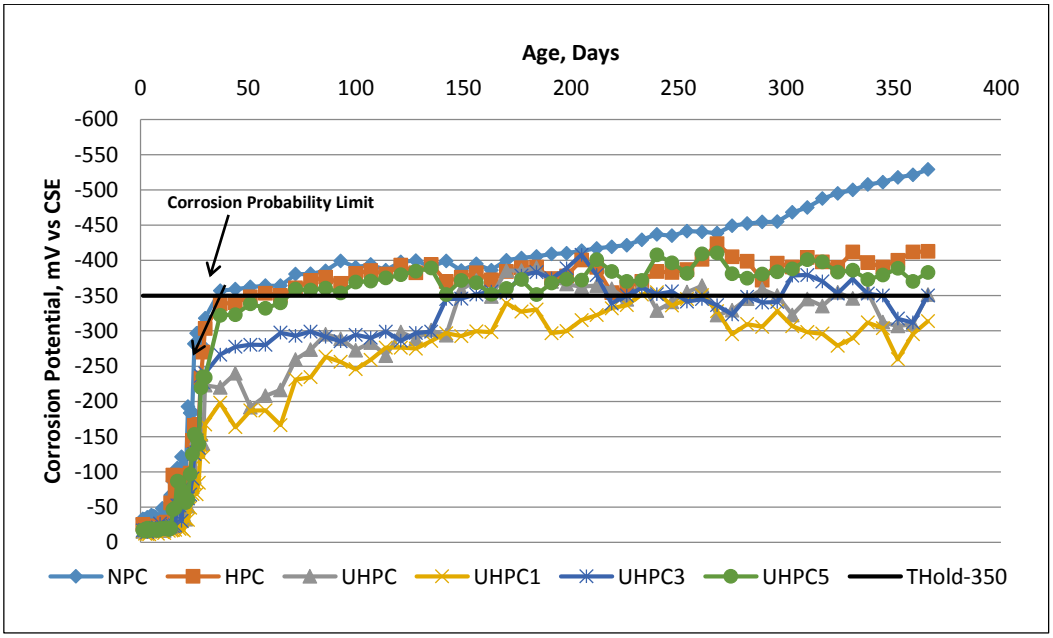

Figure 2. Corrosion potential readings of steel reinforcement embedded in NPC, HPC, UHPC and a series of nano metaclayed-UHPC with respect to age.

3.2. Corrosion monitoring by using FBG sensor

The results on strain changes for embedded steel reinforcement inside NPC, HPC, UHPC and a series of nano metaclayed-UHPC specimens corresponding to age of immersion are presented in Figure 3. The

patterns of graph showed there is sensitivity to the reflective index recorded by FBG sensors during the experiment. However, the strain change readings performance is not constant but providing valuable information on the strain change patterns. The strain changes readings recorded by FBG sensor for NPC, HPC, UHPC and a series of nano metaclayed-UHPC were considerably affected by age and different types of concrete used. A progressive shift in strain readings were observed for NPC when the specimen was exposed for 139 days. Meanwhile, the large changes in strain for HPC and UHPC5 was observed at 132 days. The change in strain for the entire concrete indicated the corrosion on the embedded steel have been started due to large changes in strain. It is notice that the corrosion readings for steel embedded in NPC specimens possess the highest possibility of corrosion potential as well as the large strain was observed until day 365. The strain change readings for UHPC1 was perfectly better in the performance. The strain changes on the surface of steel embedded in UHPC1 specimen was not as progressive and the readings are consistent till 365 days. This is proved that the expansion strain on the steel embedded in UHPC1 was small and no corrosion have been detected. Thus, it can be noted that UHPC1 specimen was found to be better in corrosion resistance due to the consistent strain change and low positive change in strain. Previous researches have been documented that the corrosion of steel bar embedded in concrete was predicted due to expansion of cross-section that calculated from the wavelength shift of the FBG [14,17]. This was confirmed by [18,30] who also stated that FBG sensors embedded on the specimen to monitor the expansion strain caused by rebar corrosion and their performances were monitored by observing the Bragg wavelength shift. Therefore, an experimental investigation in this present study shows that the FBG sensor can be confidently used for corrosion monitoring on embedded steel in concrete.

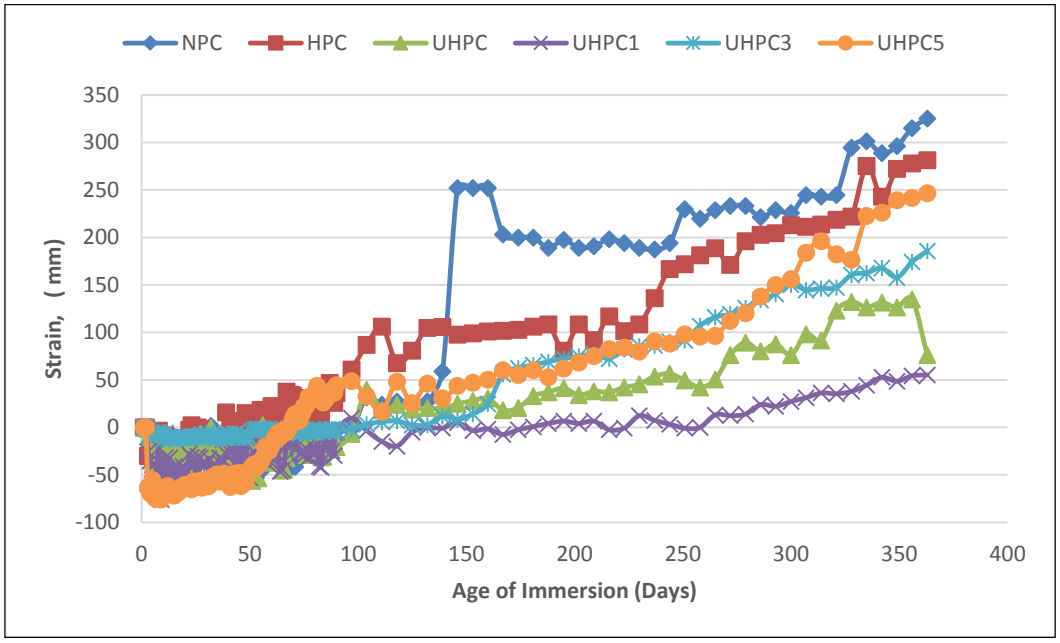

Figure 3. Strain change readings of steel reinforcement embedded in NPC, HPC, plain UHPC and a series of nano metaclayed-UHPC with respect to age.

3.3. Relationship between corrosion potential and strain changes on steel embedded in concrete

The strain changes on the embedded steel monitored using FBG sensor and the corrosion potential recorded by half-cell potential is presented. The relationship was generated by Design Expert software and the data was analyzed using response surface methodology (RSM) to relate the corrosion potential and strain changes on embedded steel in entire concrete specimens. The analysis of RSM is supported by the regression analysis and its accuracy presented by regression values (R^2). Figure 4 depicts the relationship between corrosion potential and strain changes corresponding to age for NPC, HPC, UHPC

and a series of nano metaclayed-UHPC. Based on the R^2 obtained, there is a strong and very strong relationship between corrosion potential and strain changes for the all concrete specimens. It is clearly showed that the coefficient of R^2 value generated by RSM is higher than 0.80 for all models. The R^2 obtained from RSM for NPC, HPC, UHPC, UHPC1, UHPC3 and UHPC5 models associated with corrosion potential with respect to strain changes were found to be 0.95, 0.99, 0.87, 0.93, 0.98 and 0.97, respectively. The R^2 obtained showed the positive significant and strong correlation between corrosion potential and strain changes for the entire concrete. This means that about 86.63% to 99.80% variations in strain changes can be explained by the corrosion potential on the embedded steel. The relation between corrosion potential and strain changes corresponding to age was created based on linear equation as suggested by RSM.

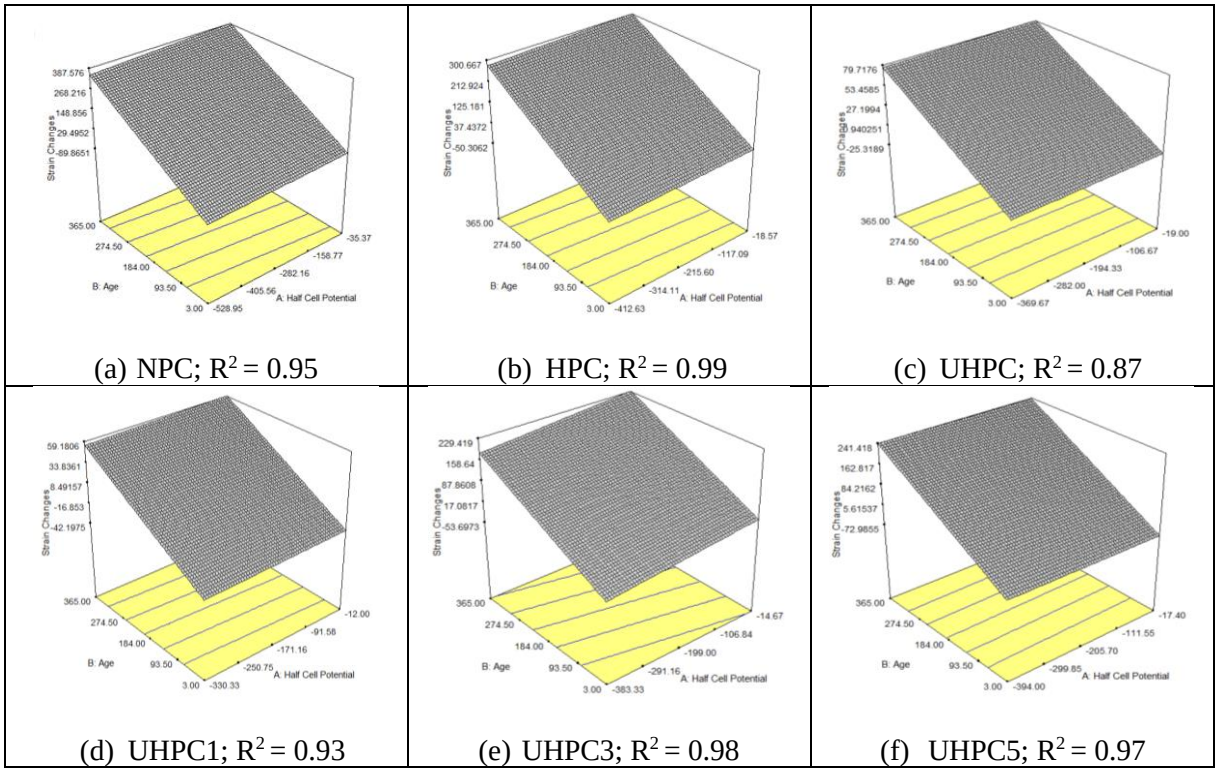

(a) NPC; $R^2 = 0.95$ (b) HPC; $R^2 = 0.99$ (c) UHPC; $R^2 = 0.87$

(d) UHPC1; $R^2 = 0.93$ (e) UHPC3; $R^2 = 0.98$ (f) UHPC5; $R^2 = 0.97$

Figure 4. Relationship between corrosion potential measured by half-cell potential and strain changes measured by FBG sensor on steel embedded in concrete.

4. Conclusions

From these findings, the conclusions can be drawn as follows:

1. The corrosion potential recorded by half-cell potential for embedded steel showed the increment in negative values of potential with increasing the day of exposure. It is noticeably that the corrosion potential of steel embedded in NPC extremely higher corrosion probability as compared to those of HPC, UHPC and nano metaclayed-UHPC.
2. The strain changes recorded from FBG observed that a progressive shifted Bragg wavelength. A large strain changes on steel surface was recorded for steel embedded in NPC and indicating the detection on corrosion possibility of the steel to corroded.
3. It is demonstrated that inclusion of 1% nano metaclay in UHPC was significantly affect the performance and attributed to positive effect on corrosion resistance for embedded steel measured by using both technique.
4. It revealed that the corrosion potential of embedded steel in concrete recorded by half-cell potential can be explained by the variations in strain changes recorded by FBG sensor.

References

[1] Zhang Y, Fan Y, Li H and Wu X 2010 Study on evaluation method of corroded reinforcing steel *J. Appl. Mech. Mater.* **26-28** p 1184-1189
[2] Kelly R G and Jones S H 1999 Development of an embeddable micro instrument for corrosivity monitoring in concrete *Final Contract Rep.* (Virginia Transportation Research Council)
[3] Song H W and Saraswathy V 2007 Corrosion monitoring of reinforced concrete structures: A review *Int. J. Electrochem. Sci.* **2** p 1-28
[4] Sharma S and Mukherjee A 2011 Monitoring corrosion in oxide and chloride environments using ultrasonic guided waves *J. Mater. Civil Eng.* **23** 2 p 207-211
[5] Angst U M, Elsener B, Larsen C K and Vennesland Ø 2011 Chloride induced reinforcement corrosion: Electrochemical monitoring of initiation stage and chloride threshold values *Corr. Sci.* **53** p 1451-1464
[6] Reou J S and Ann K Y 2009 Electrochemical assessment on the corrosion risk of steel embedment in OPC concrete depending on the corrosion detection techniques *Mater. Chem. Phys.* **113** p 78-84
[7] Muhammad W and Raja R H 2013 Experimental investigation of re-corrosion phenomenon in simulated repaired steel reinforced self-consolidating concrete structures *Int. J. Electrochem. Sci.* **8** p 1678-1690
[8] Sadowski L 2013 Methodology for assessing the probability of corrosion in concrete structure on the basis of half-cell potential and concrete resistivity measurement *The Sci. World J.* ID 714501(Hindawi Publishing Corporation)
[9] Mao J, Chen J, Cui L, Jin W, Xu C and He Y 2015 Monitoring the corrosion process of reinforced concrete using BOTDA and FBG sensors *Sensors* **15** p 8866-8883
[10] Majumder M, Gangopadhyay T K, Chakraborty A K, Dasgupta K and Bhattacharya D K 2008 Fibre Bragg gratings in structural health monitoring: Present status and applications. *Sens. Act. A* **147** p 150-164
[11] Zrelli A, Bouyahi M and Ezzedine T 2016 Simultaneous monitoring of humidity and strain based on Bragg sensor. *J. Optic* **127** p 7326-7331
[12] Montanini R and Pirrotta S 2006 A temperature-compensated rotational position sensor based on fibre Bragg gratings *Sens. Act. A* **132** p 533-540
[13] Sidek O, Kabir, S and Afzal M H 2011 Fiber optic-based sensing approach for corrosion detection *PIERS Proc.* p 642-646 September 12-16 Suzhou China
[14] Chen W and Dong X 2012 Modification of the wavelength - strain coefficient of FBG for the prediction of steel bar corrosion embedded in concrete *Opt. Fiber Technol.* **18** p 47-50
[15] Shi X, Xie N, Fortune K and Gong J 2012 Durability of steel reinforced concrete in chloride environments: An overview *Constr. Build. Mater.* **30** p 125-138
[16] Hu W, Cai H, Yang M, Tong X, Zhou C and Chen W 2011 Fe-C-coated fibre Bragg grating sensor for steel corrosion monitoring *Corr. Sci.* **53** p 1933-1938
[17] Gao J, Wu J, Li J and Zhao X 2011 Monitoring of corrosion in reinforced concrete structure using Bragg grating sensing. *NDT & E Int.* **44** p 202-205
[18] Tan C H, Shee Y G, Yap B K and Mahamd Adikan F R 2016 Fiber Bragg grating based sensing system: Early corrosion detection for structural health monitoring *Sens. Act. A* **246** p 123-128
[19] Al Handawi K, Vahdati N, Rostron P, Lawand L and Shiryayev O Strain based FBG sensor for real-time corrosion rate monitoring in pre-stressed structure *Sens. Act. B* **236** p 276-285
[20] Almubaied O, Chai H K, Islam M R, Lim K S, Tan C G 2017 Monitoring corrosion process of reinforced concrete using FBG strain sensor *IEEE Trans. on Instr. and Measure.* **66** 8 p 2148

-2155
[21] Borosnyói A 2016 Long term durability performance and mechanical properties of high performance concretes with combined use of supplementary cementing materials *Cons. Build. Mater.* **112** p 307-324
[22] Otieno M, Beushausen H and Alexander M 2016 Chloride-induced corrosion of steel in cracked concrete – Part I : Experimental studies under accelerated and natural marine environments *Cem. & Concr. Res.* **79** p 373-385
[23] Wang X, Yu R, Shui Z, Song Q and Zhang Z 2017 Mix design and characteristics evaluation of an eco-friendly ultra-high performance concrete incorporating recycled coral based materials *J. Cleaner Product.* **165** p 70-80
[24] Kim Y Y, Kim J M, Bang j W and Kwon S J 2014 Effect of cover depth, w/c ratio and crack width on half-cell potential in cracked concrete exposed to salt sprayed condition *Cons. Build. Mater.* **54** p 636-645
[25] Yodsudjai W and Pattarakittam T 2017 Factors influencing half-cell potential measurement and its relationship with corrosion level *Measurement* **104** p 159-168
[26] Angst U M and Polder R 2014 Spatial variability of chloride in concrete within homogeneously exposed area *Cem. Concr. Res.* **56** p 40-51
[27] Nithya P S and Mathew G Effect of fly ash on corrosion potential of steel in concrete *Int. Res. J. Eng. Technol.* **3** 9 p 860-864 e-ISSN 2395-0056
[28] Hossain M M, Karim M R, Hasan M, Hossain M K and Zain M F M 2016 Durability of mortar and concrete made up of pozzolans as a partial replacement of cement: A review *Cons. Build. Mater.* **116** p 128-140
[29] Minu R R and Mathew G 2016 Effect of GGBS on corrosion potential of steel in concrete *Int. Res. J. Eng. Technol* **3** 9 p 690-694 e-ISSN 2395-0056
[30] Ren L, Jiang T, Li H N and Yi T H 2016 The study of pipeline corrosion monitoring using fiber optic sensing technique *The 2016 Struc. Congr. (Structures16)* Jeju Island Korea, Aug. 28-Sept. 1